



Published in final edited form as:

J Pathol. 2017 November ; 243(3): 376–389. doi:10.1002/path.4958.

High-mobility group box 1 released by autophagic cancer-associated fibroblasts maintains the stemness of luminal breast cancer cells

Xi-Long Zhao¹, Yong Lin¹, Jun Jiang², Zhuo Tang¹, Shuai Yang¹, Lu Lu¹, Yan Liang^{1,2}, Xue Liu¹, Jiao Tan¹, Xu-Gang Hu¹, Qin Niu¹, Wen-Juan Fu¹, Ze-Xuan Yan¹, De-Yu Guo¹, Yi-Fang Ping¹, Ji Ming Wang³, Xia Zhang¹, Hsiang-Fu Kung^{1,*}, Xiu-Wu Bian^{1,*}, Xiao-Hong Yao^{1,*}

¹Institute of Pathology and Southwest Cancer Centre, Southwest Hospital, Third Military Medical University, Chongqing, PR China

²Breast Disease Centre, Southwest Hospital, Third Military Medical University, Chongqing, PR China

³Cancer and Inflammation Program, Center for Cancer Research, National Cancer Institute at Frederick, Frederick, MD, USA

Abstract

Cancer stem cells/cancer-initiating cells (CICs) and their microenvironmental niche play a vital role in malignant tumour recurrence and metastasis. Cancer-associated fibroblasts (CAFs) are major components of the niche of breast cancer-initiating cells (BCICs), and their interactions may profoundly affect breast cancer progression. Autophagy has been considered to be a critical process for CIC maintenance, but whether it is involved in the cross-talk between CAFs and CICs to affect tumourigenesis and pathological significance has not been determined. In this study, we found that the presence of CAFs containing high levels of microtubule-associated protein 1 light chain 3 (LC3II), a marker of autophagosomes, was associated with more aggressive luminal human breast cancer. CAFs in human luminal breast cancer tissues with high autophagy activity enriched BCICs with increased tumourigenicity. Mechanistically, autophagic CAFs released high-mobility group box 1 (HMGB1), which activated its receptor, Toll-like receptor (TLR) 4, expressed by luminal breast cancer cells, to enhance their stemness and tumourigenicity. Furthermore, immunohistochemistry of 180 luminal breast cancers revealed that high LC3II/TLR4 levels predicted an increased relapse rate and a poorer prognosis. Our findings demonstrate that autophagic CAFs play a critical role in promoting the progression of luminal breast cancer through

*Correspondence to: Xiao-Hong Yao or Hsiang-Fu Kung or Xiu-Wu Bian, Institute of Pathology and Southwest Cancer Center, Southwest Hospital, Third Military Medical University, Chongqing 400038, PR China. yxh15@hotmail.com; hfkung@163.com; bianxiuwu@263.net.

Author contributions statement

The authors contributed in the following way: X-LZ, YL: performed most of the experiments and wrote the manuscript; LL, SY: performed the lentivirus and adenovirus infection; XL, JJ, YL, TJ: collected the clinical specimens; X-GH, Z-XY, QN: prepared the reagents; W-JF: performed the western blotting; X-HY, Y-FP, D-YG: performed the immunohistochemical scoring; X-HY, X-WB: performed data analysis; J-MW, XZ: edited and revised the manuscript; X-HY, H-FK, X-WB: designed the study, revised the manuscript, and provided administrative management.

No conflicts of interest were declared.

an HMGB1–TLR4 axis, and that both autophagy in CAFs and TLR4 on breast cancer cells constitute potential therapeutic targets.

Keywords

autophagy; breast cancer-initiating cell (BCIC); cancer-associated fibroblast (CAF); high-mobility group box 1 (HMGB1); Toll-like receptor 4 (TLR4)

Introduction

Luminal breast cancer represents two-thirds of all breast cancers. Despite adjuvant endocrine therapy and chemotherapy for patients after surgery, both early and late relapses still occur. Current anticancer therapy is aimed at cancer cells of unspecified types, although solid tumours represent an organized, heterogeneous cell population [1]. The complicated cell–cell interactions that form the tumour microenvironment (or niche) involve a small population of cells termed cancer stem cells or cancer-initiating cells (CICs) [2]. Both CICs and their niche play major roles in cancer recurrence, metastasis, and drug resistance [3–5]. Thus, specifically targeting CICs and their microenvironment has been suggested as a new strategy for anticancer therapy [6–8].

CICs have been identified as being critical for tumour initiation and drug resistance in breast cancer [4,9]. Breast cancer-initiating cells (BCICs), characterized by expression of aldehyde dehydrogenase (ALDH) [10], reside in a niche containing cancer-associated fibroblasts (CAFs). CAFs are the predominant components of the breast cancer microenvironment, and play roles in the occurrence and progression of breast cancer [11,12]. Co-culture with cancer cells has revealed that CAFs support CIC enrichment in breast and lung cancer [13,14]. However, the mechanisms by which CAFs interact with CICs and the pathological significance remain elusive.

Recently, autophagy has been reported to support the survival and maintenance of CICs in breast [15,16], brain [17] and colon [18] cancer. In addition to cancer cells, CAFs, vascular endothelial cells and other stromal cells also respond to perturbations in the tumour microenvironment, probably because of the inadequate supply of blood and depletion of nutrients. Recent research has revealed that, when deprived of oxygen, nutrients, and growth factors, cells maintain their survival through autophagic degradation of misfolded proteins and damaged organelles via regulation of autophagy-related gene (*ATG*) products. Moreover, certain leaderless proteins need autophagic membranes for efficient envelopment and exocytosis for unconventional secretion, named autosecretion [19–21]. CAFs from breast cancer have autophagic activity [22]; however, it is unclear whether any cytokines secreted by CAFs in the niche through autophagy-based unconventional secretion are involved in the cross-talk between CICs and CAFs to promote tumourigenesis and self-renewal of CICs.

In an effort to elucidate the interaction between CAFs and breast cancer cells, we identified autophagy protein microtubule-associated protein 1 light chain 3 (LC3II; also known as MAP1LC3B) in luminal human breast cancer. Evaluation of the expression and clinical

relevance of LC3II revealed important contributions of autophagic CAFs to breast cancer stemness and patient outcomes.

Materials and methods

Human breast cancer specimens

Human breast cancer specimens were obtained from 431 patients after surgical resection at the First Affiliated Hospital of Third Military Medical University, Chongqing, China from 2006 to 2007, with approval from the Institutional Ethics Committee. All patients provided informed consent. The surgical specimens were formalin-fixed, sectioned, stained with haematoxylin and eosin, and examined by microscopy. Patient information is summarized in supplementary material, Table S1. The histological diagnosis was reached on the basis of the World Health Organization classification standard and St Gallen consensus panel in 2013 [23]. An independent cohort of 641 patient specimens from The Cancer Genome Atlas (TCGA) database (<https://tcga-data.nci.nih.gov/tcga>; TCGA BRCA exp HiSeqV2 PANCAN-2014-05-02) was utilized to analyse the relationship between ALDH 1 family member A1 (ALDH1A1) and receptors for high-mobility group box 1 (HMGB1).

Cell culture

Human breast CAFs were harvested from freshly resected tumours of luminal breast cancer patients who underwent surgery. The protocol for tissue collection was approved by the Ethics Committee, and informed consent was obtained from all patients enrolled. The primary cells used were passaged fewer than five times after recovery. Human breast cancer cell lines (MCF-7 and T47D) were obtained from the American Type Culture Collection (Manassas, VA, USA), and maintained in RPMI-1640 supplemented with 10% fetal bovine serum (Invitrogen, Carlsbad, CA, USA). Cells used were passaged for <3 months after recovery.

Reagents

Human recombinant HMGB1 was from Chimerigen Laboratories (CHI-HR-200; San Diego, CA, USA). Lipopolysaccharide (LPS) was from Beyotime (S1732; Jiangsu, China). Glycyrrhizic acid ammonium salt (GL) was from Sigma-Aldrich (#01250570; St Louis, MO, USA). TAK-242 was from Cayman Chemical (243984-11-4; Ann Arbor, MI, USA).

Autophagy assay

For observation of autophagosomes, CAFs were transfected with Ad-mGFP-LC3 (hanbio20130521-Adpremade-002; HANBIO, Shanghai, China) in accordance with the instruction manual. After culture in serum-free medium for 24 h, the accumulation and distribution of CAFs containing mGFP-LC3 puncta were examined under confocal microscopy 48 h after transfection. CAFs with mGFP-LC3 puncta were counted under 50 randomly selected separate $\times 400$ fields. The data presented are from one representative experiment out of at least three independent repeats.

Lentivirus and adenovirus infection

CAFs were infected with concentrated *ATG5*-knockdown (KD)-eGFP lentivirus or empty control lentivirus vectors (NBFW-lenti-3299; OBIO Company, Shanghai, China), and were then selected and enriched by use of a FACS Aria II (BD Biosciences, San Jose, CA, USA). Lipofectin 2000 (Invitrogen) was used for cell transfection.

Conditioned medium (CM) production

CAFs at ~80% confluency and breast cancer cells at ~70% confluency in flasks were washed with phosphate-buffered saline (PBS), and then incubated for 48 h in serum-free RPMI-1640 (Invitrogen). CM was collected and filtered through a 0.22- μ m filter (SLGP033RB; Merck Millipore, Danvers, MA, USA) to remove cellular debris.

Sphere-forming assay

The sphere-forming assay was performed as described previously [24]. Cells were plated in ultra-low-attachment plates (Corning, New York, NY, USA), and suspended in serum-free Dulbecco's modified Eagle's medium-F12 (Invitrogen) with 20 ng/ml epidermal growth factor, 10 ng/ml basic fibroblast growth factor, 5 μ g/ml insulin, and 0.4% bovine serum albumin (Sigma-Aldrich). After 14 days, spheres with diameters of 75 μ m were counted by microscopy [25] (see supplementary material, Supplementary materials and methods).

Flow cytometry and fluorescence-activated cell sorting

ALDH activity in breast cancer cells was measured with an ALDEFLUOR assay kit (#01700; Stem Cell Technologies, Durham, NC, USA). Cells were suspended in ALDEFLUOR assay buffer containing the ALDH substrate BODIPY-aminoacetaldehyde. As a control, the cells were treated with diethylaminobenzaldehyde, a specific ALDH inhibitor. Single-cell suspensions of each breast cancer cell line were counted, and the cells were sorted with a FACS Aria II (BD Biosciences) after incubation with anti-CD284 [Toll-like receptor (TLR) 4]-allophycocyanin (130-096-236; Miltenyi Biotec, Bergisch Gladbach, Germany).

Enzyme-linked immunosorbent assay (ELISA), western blotting, and quantitative reverse transcription polymerase chain reaction (qRT-PCR)

Detailed procedures and materials are described in supplementary material, Supplementary materials and methods. Western blotting was performed as described previously [26]. The primer sequences for quantitative RT-PCR are listed in supplementary material, Table S2.

Immunohistochemistry (IHC)

The procedure was conducted with the Dako REAL EnVision Detection System (Dako, Glostrup, Denmark) in accordance with the manufacturer's instructions. Formalin-fixed paraffin-embedded human breast cancers were sectioned at 4 μ m. The primary antibodies were anti-LC3II (anti-LC3II/MAP1 LC3II, 1:200, NB100-2220; Novus Biologicals, Littleton, CO, USA), anti-ATG5 (1:100, ab108327; Abcam, Cambridge, UK), anti-TLR4 (1:100, ab22048; Abcam), anti-ALDH1A1 (1:100, ab56777; Abcam), anti-ALDH 1 family member A3 (ALDH1A3) (1:400, ab129815; Abcam), anti-oestrogen receptor, anti-

progesterone receptor, anti-human epidermal growth factor 2 (ready-to-use for IHC, DKT-3022; MXB, Fuzhou, China), and anti-Ki67 (1:100, MAB-0672; MXB), and were independently assessed by two pathologists according to the staining intensity and the percentage of positive tumour cells, as previously described [27] (see supplementary material, Supplementary materials and methods for details of scoring and double-labelling).

Immunofluorescence microscopy

Isolated CAFs were fixed in 4 % paraformaldehyde and blocked with normal goat serum. Rabbit polyclonal anti-fibroblast activation protein (FAP) (1 µg/ml, ab28246; Abcam) and mouse monoclonal anti-cytokeratin (1:25, M7019; Dako) were used as primary antibodies, and were detected by CY3-conjugated goat anti-rabbit IgG (1:50, BA1032; Boster Biotech, Wuhan, China) and fluorescein isothiocyanate (FITC)-conjugated goat anti-mouse IgG (1:50, BA1101; Boster Biotech). Double immunofluorescence staining was used to detect the coexpression of HMGB1 (1:700, ab18256; Abcam) and LC3II (1:90, M152-3; MBL, Nagoya, Japan) in primary CAFs. After staining with primary antibodies by the use of CY3-conjugated goat anti-rabbit IgG (1:50, BA1032; Boster Biotech), the samples were incubated with mouse monoclonal anti-LC3II for another 12 h and detected by FITC-conjugated goat anti-mouse IgG (1:50, BA1101; Boster Biotech). All samples were examined under a laser confocal scanning microscope (LSM780NLO; Zeiss, Jena, Germany).

Tumour xenografts

Animal care was provided in accordance with the Guide for the Care and Use of Laboratory Animals. Four-week-old female NOD-SCID mice (Laboratory Animal Centre, Third Military Medical University, Chongqing, China) were randomized into different groups for mammary fat pad injection of tumour cells. After 40 days, tumour volume (T_v) was calculated with the formula $T_v = (L \times W^2)/2$, where L = length and W = width [28]. To study the interaction between CAFs and breast cancer cells, MCF-7 cells (5×10^6) mixed with shCtrl-CAF3 or shATG5-CAF3 (10×10^6) at a ratio of 1:2 were injected into the right side of the mammary fat pad (one injection/mouse) in a 1:1 mixture of PBS and Matrigel (356234; BD Biosciences). To investigate the role of TLR4 in the interaction between CAFs and breast cancer cells, isolated TLR4⁺ MCF-7 cells (1×10^5) and TLR4⁻ MCF-7 cells (1×10^5) were, respectively, mixed with or without shCtrl-CAF3 and shATG5-CAF3 (2×10^5) (see Results), and were injected into the mammary fat pad.

Statistical analysis

All experiments were performed at least three times. Data are presented as the mean \pm standard deviation or 95% confidence interval or as otherwise indicated. Individual group means were compared by the use of a two-tailed Student's *t*-test or one-way ANOVA to determine significance. Linear regression and the *F*-test were used to determine the significance of TCGA data. Associations between variables were assessed with the chi-square test or Kruskal–Wallis test. Kaplan–Meier analysis was used to estimate the overall survival (OS) rate or the relapse-free survival (RFS) rate of patients. A Cox proportional hazard regression model was used to determine the influence of various parameters on patients' survival in univariate and multivariable analyses. Analyses were performed with

SPSS software version 10.0 (SPSS, Chicago, IL, USA). $P < 0.05$ was considered to be statistically significant.

Results

Autophagy activity in CAFs is associated with a poor prognosis of luminal breast cancer patients

To determine the contribution of autophagy activity of CAFs to breast cancer progression, the autophagosome marker LC3II was examined in 431 human breast cancer specimens. For Kaplan–Meier analysis of correlation with LC3II level, 246 samples were designated as LC3II^{high} or LC3II^{low} (Figure 1A) (57 patients were removed from 303 luminal breast cancer patients for being aged >75 years with <3 months of follow-up and clinical stage 4). Patients with higher LC3II levels in CAFs showed significantly poorer OS and RFS (Figure 1B; supplementary material, Figure S1). However, LC3II levels in cancer cells were not correlated with OS and RFS (supplementary material, Figure S2), although both tumour size and grade were poor indicators of patient prognosis ($P = 0.047$ and $P = 0.042$, respectively; supplementary material, Table S3). High expression of LC3II in CAFs was correlated with high cancer relapse rates (Figure 1C, left panel) and lymph node metastasis (LNM) (Figure 1C, middle panel) (supplementary material, Table S4). Moreover, LC3II in CAFs was expressed at higher levels in luminal breast cancer patients with shorter OS (Figure 1C, right panel). High expression of BECN1 in CAFs was also correlated with poor prognosis (supplementary material, Figure S3 and Table S5). ALDH1⁺ CICs in breast cancer have recently been shown to be critical for cancer recurrence and metastasis [9–12]. ALDH1A1^{high} and ALDH1A3^{high} breast cancer cells were observed around LC3II^{high} CAFs in luminal breast cancer (Figure 1D, E). High expression of LC3II in CAFs was correlated with the levels of ALDH1A1 and ALDH1A3 in cancer cells (supplementary material, Table S4). These results suggest that autophagy activity in CAFs may support BCICs and contribute to the poor prognosis of luminal breast cancer.

BCIC enrichment by autophagic CAFs in luminal breast cancer

To investigate the interaction between autophagic CAFs and breast cancer cells, primary CAFs were isolated from human luminal breast cancer without presurgical therapy. Primary CAFs were fibroblast-like and consistently expressed α -smooth muscle actin and FAP, but not cytokeratin (supplementary material, Figure S4). We used serum-free media to induce autophagy in CAFs obtained from three individuals (CAF1, CAF2, and CAF3), and found that the levels of autophagy-related gene mRNAs, including those of *ATG5*, *ATG12*, and *ATG7*, as well as *BECN1*, were different among CAFs, whereby CAF3 expressed the highest levels of autophagy-related genes (Figure 2A).

The overexpression of GFP–LC3 [in which green fluorescent protein (GFP) is expressed as a fusion protein at the N-terminus of LC3] is widely used to subjectively measure autophagy [29]. We generated CAFs containing an mGFP–LC3 reporter, and counted GFP-positive punctate structures to quantify relative levels of autophagy by fluorescence microscopy. CAFs from CAF3 containing mGFP–LC3 cultured in serum-free medium showed the highest number of green fluorescent spots (Figure 2B), suggesting that autophagy activity is

different among CAFs. We then used supernatants from CAFs in serum-free medium as CM (CM-CAF3) to culture a luminal breast cancer cell line, MCF-7. CM-CAF3 caused the highest increase in mRNA levels of the stem cell markers *POU5F1* (also called OCT4), *SOX2*, and *NANOG* (Figure 2C). There was also greater enrichment of ALDH⁺ BCICs in MCF-7 cells cultured with CM-CAF3 (Figure 2D); however, we found that only 0.03% or 0.07% CD44⁺/CD24⁻ MCF-7 cells were detected when they were cultured with full medium or CM-CAF3, respectively (data not shown).

To investigate the role of autophagy in CAFs in regulating the stemness maintenance of BCICs, we knocked down a key autophagy gene, *ATG5*, with short hairpin RNA (shRNA) in CAFs (supplementary material, Figure S5). CM collected from *ATG5*-KD CAFs (CM-sh*ATG5*-CAF3) showed reduced capacity to enrich ALDH⁺ BCICs in the luminal breast cancer cell lines MCF-7 and T47D (Figure 2E, F). The sphere-forming capabilities (Figure 2G) and levels of the stemness markers *POU5F1*, *SOX2* and *NANOG* were also reduced in MCF-7 and T47D cells cultured with CM-sh*ATG5*-CAF3 (Figure 2H). Furthermore, CAFs with KD of *ATG5* (sh*ATG5*-CAF3) significantly decreased the tumorigenicity of MCF-7 cells in NOD-SCID mice as compared with MCF-7 cells in the presence of control CAFs (shCtrl-CAF3) (Figure 2I). These results indicate that factors released by autophagic CAFs may increase the self-renewal of BCICs and the tumorigenicity of luminal breast cancer cells.

Release of HMGB1 by autophagic CAFs

Some leaderless proteins, such as HMGB1, interleukin (IL)-18, and IL-1 β , are released by an autophagy-based unconventional secretion (autosecretion) process (Figure 3A) in mammalian cells [19–21]. We therefore tested whether autophagic CAFs might release leaderless proteins. Serum starvation promoted CAF3 to release HMGB1, but not IL-1 β and IL-18, as detected by ELISA (Figure 3B). As HMGB1 is a nuclear protein and functions as a proinflammatory cytokine when released into extracellular compartments [30], we visualized its translocation in CAFs. After autophagy induction in CAFs, HMGB1 was released from the nuclei into the extracellular compartment as shown by immunofluorescence and ELISA (Figure 3C, D), presumably by exocytosis. Interestingly, HMGB1 and LC3II were co-localized in autophagic CAFs (Figure 3E; supplementary material, Figure S6), suggesting that autophagic vesicles and HMGB1 are physically associated. KD of *ATG5* in CAFs diminished HMGB1 secretion, and instead caused its retention intracellularly (Figure 3F, G). In human luminal breast cancer specimens with high levels of LC3II in CAFs, HMGB1 levels in the nuclei and cytoplasm of tumour cells were significantly diminished (Figure 3H, Case 1). However, in specimens with low levels of LC3II in CAFs, HMGB1 accumulated in the nuclei and cytoplasm of cancer cells (Figure 3H, Case 2), suggesting that the expression of LC3II in CAFs is inversely correlated with HMGB1 in cancer cells. These results suggest that HMGB1 is secreted by autophagic CAFs into the tumour microenvironment to maintain the stemness of BCICs in luminal breast cancer.

Requirement of HMGB1 for self-renewal of BCICs

To examine whether HMGB1 released by CAFs promotes the stemness of BCICs, MCF-7 and T47D cells were treated with exogenous HMGB1. To the best of our knowledge, the physiological HMGB1 level in human breast cancer specimens remains unknown. Nevertheless, the concentration of HMGB1 used in the experiment shown in Figure 4A was similar to that in the previous study using HMGB1 as a cytokine for cellular functional assays [31]. Quantitative RT-PCR showed that HMGB1, especially 1 µg/ml HMGB1, significantly increased the mRNA levels of the stemness marker genes *NANOG*, *SOX2* and *POU5F1* in breast cancer cells (Figure 4A). Flow cytometry revealed significant increases in the numbers of ALDH⁺ cells in MCF-7 and T47D cells cultured with 1 µg/ml HMGB1 (Figure 4B; supplementary material, Figure S7A). The sphere-forming capabilities of MCF-7 and T47D cells were also increased after treatment with 1 µg/ml HMGB1 (Figure 4C). We then used GL to attenuate HMGB1 activity in the medium of autophagic CAFs. GL, a natural triterpene glycoconjugate derived from the root of liquorice (*Glycyrrhiza glabra* L.), binds to both HMG boxes of HMGB1 to inhibit its activity, but may not be a specific HMGB1 inhibitor [30–34]. GL abolished the capacity of autophagic CAFs to increase the proportion of ALDH⁺ cells (Figure 4D; supplementary material, Figure S7B) and sphere formation by MCF-7 and T47D cells (Figure 4E). These results confirm the ability of HMGB1 released by autophagic CAFs to promote the stemness of luminal breast cancer cells.

Activation of TLR4 on luminal breast cancer cells by HMGB1

As HMGB1 is a ligand for several receptors such as TLR4, TLR2, TLR9, and RAGE, we analysed the relationship between receptor expression pattern and ALDH1A1 in breast cancer by using TCGA data. Pearson correlation analysis showed a significant correlation ($r^2 = 0.586$, $P < 0.01$) between the levels of ALDH1A1 and TLR4 in luminal breast cancer specimens (Figure 5A). Isolated TLR4⁺ MCF-7 cells expressed a high level of *ALDH1A1* (Figure 5B), and treatment with HMGB1 enhanced the expression of stemness markers such as *POU5F1*, *SOX2* and *NANOG* in TLR4⁺ MCF-7 cells (Figure 5C). Treatment with LPS, a canonical ligand of TLR4, also increased the proportion of ALDH⁺ BCICs in luminal breast cancer cells (supplementary material, Figure S8A, B), suggesting that TLR4 expressed by luminal breast cancer cells is functional. TAK-242, a TLR4 antagonist [35], reduced the proportion of ALDH⁺ cells (Figure 5D; supplementary material, Figure S8C) and the expression of the stemness markers *POU5F1*, *SOX2* and *NANOG* (Figure 5E) in luminal breast cancer cells cultured with CM-CAF3. To evaluate cross-talk between autophagic CAFs and TLR4⁺ BCICs, isolated TLR4⁺ and TLR4⁻ MCF-7 cells were co-injected with shCtrl-CAF3 or sh*ATG5*-CAF3 into the mammary pads of NOD-SCID mice. CAFs with intact ATG5 (shCtrl-CAF3) maintained the tumorigenicity of TLR4⁺ MCF-7 cells but not that of TLR4⁻ cells (Figure 5F). These results confirm the capacity of CAFs to enhance the stemness of BCICs and tumorigenesis of luminal breast cancer cells through an HMGB1–TLR4 axis.

Correlation between LC3II/TLR4 levels in luminal human breast cancer and poor prognosis of patients

We then examined patient specimens ($n = 303$) of luminal breast cancer for the clinical relevance of LC3II in CAFs and TLR4 on cancer cells to tumour progression (supplementary material, Table S6). For Kaplan–Meier analysis, 246 patients with luminal breast cancer were designated as TLR4^{high} or TLR4^{low} (Figure 6A). High TLR4 levels in cancer cells were associated with poorer OS and RFS (Figure 6B; $P = 0.06$ and $P = 0.025$). For combined analysis of LC3II and TLR4, we matched a high level of TLR4 in breast cancer cells with a high level of LC3II in CAFs (TLR4^{high}/LC3II^{high}, $n = 87$) and a low level of TLR4 in breast cancer cells with a low level of LC3II in CAFs (TLR4^{low}/LC3II^{low}, $n = 121$) (supplementary material, Table S7) (95 patients were removed from 303 patients because they did not meet the TLR4^{low}/LC3II^{low} and TLR4^{high}/LC3II^{high} criteria). Patients with TLR4^{high}/LC3II^{high} tumours had higher rates of relapse and LNM (supplementary material, Table S7), and significantly poorer OS and RFS, than those with TLR4^{low}/LC3II^{low} tumours (Figure 6C) (28 patients were removed from 208 patients for being aged >75 years with <3 months of follow-up and clinical stage 4). Cox proportional hazards regression further demonstrated that combined expression of LC3II and TLR4 in luminal breast cancer provides a prognostic parameter for OS [hazard ratio (HR) 7.059, 95% confidence interval (CI) 1.126–44.245; $P = 0.037$; supplementary material, Table S8] and RFS (HR 2.735, 95% CI 1.111–6.734; $P = 0.029$; supplementary material, Table S9) of luminal breast cancer patients.

Discussion

In the tumour microenvironment, autophagy in cancer cells and CAFs is activated by an inadequate supply of blood and nutrients, and by anticancer treatment-induced stress. The role of autophagy in cancer progression is complex, and is probably dependent on the heterogeneity of tumours [36]. Recently, autophagy was shown to be required for CICs to support the survival and maintenance of stem-like properties in breast, brain and colon cancers [15–17,37]. In addition to cancer cells, CAFs acting as the main stromal components in breast cancer also respond to perturbations of the tumour microenvironment. In this study, we found that CAFs in human luminal breast cancer tissues containing a high level of LC3II, a protein involved in autophagosome formation, were correlated with a poor prognosis of patients. CAFs with different autophagic states induce different rates of progression in luminal breast cancer. Furthermore, to study the effect of CAFs' autophagy on breast cancer progression *in vivo*, we knocked down *ATG5* in CAFs, and transplanted both CAFs and MCF-7 to the mammary pad of NOD-SCID mice. Usually, MCF-7 xenografts require oestrogen pellets to establish tumours [38,39]. Here, we focused on how CAFs promote the tumorigenicity of MCF-7 cells, and so did not use oestrogen pellets. Our research showed that CAFs promoted the tumorigenicity of MCF-7 cells in mice, and that *ATG5* depletion in CAFs significantly decreased tumour growth, indicating that autophagic CAFs increase the tumorigenicity of luminal breast cancer cells. However, the mechanisms of autophagy occurring in CAFs are unclear.

Certain leaderless proteins require autophagic membranes for efficient envelopment and exocytosis as a pathway of unconventional secretion [19–21]. The role of autophagy in protein secretion and trafficking is recognized as a function of the autophagic machinery to expand the immediate sphere of influence from intracellular compartments to extracellular environments. One of the major breakthroughs in this area is the recognition that a subset of unconventionally secreted cytosolic proteins, such as HMGB1, IL-18, and IL-1 β [20,36,40], lack leader peptides and therefore cannot enter the endoplasmic reticulum-to-Golgi secretory pathway. However, it has been unclear whether mediators released by CAFs in the tumour niche through autophagy-based unconventional secretion contribute to the self-renewal of BCICs and tumourigenesis. Our findings represent a major advance in understanding autophagy-based unconventional secretion of HMGB1 by CAFs to regulate the self-renewal of BCICs in luminal breast cancers. HMGB1 has been reported to translocate from the nucleus to the cytoplasm to take part in autophagosome formation during starvation [41], oxidative stress, and cancer chemotherapy [42]. Our study reveals that LC3II co-localizing with HMGB1 elevates HMGB1 exocytosis in CAFs after autophagy induction.

HMGB1 is a nuclear protein that binds to DNA for gene transcription. When released into extracellular compartments, HMGB1 acts as a proinflammatory cytokine by interacting with cell membrane receptors, including TLR4 [41–45]. The effect of HMGB1 on cancer progression is complicated by its paradoxical dual activities [44,46–48]. In some cancers, HMGB1 is pro-tumourigenic, favouring tumour growth and invasion through its chemotactic and growth factor activity [47]. However, HMGB1 may promote genome stability and therefore inhibit tumour growth [48]. Our study demonstrates that HMGB1 released by autophagic CAFs activates TLR4 on luminal breast cancer cells to promote stemness and tumourigenicity. Thus, in addition to its proinflammatory activity, HMGB1 released by autophagic CAFs is critical for luminal breast cancer development and progression.

Breast cancer is heterogeneous, and luminal breast cancer (including luminal A and luminal B) is the main subtype [49,50]. The success of personalized therapy has been demonstrated by the development of anti-oestrogens for luminal breast cancers. However, despite advances in therapeutic development, some patients with luminal breast cancer develop drug resistance accompanied by cancer relapse. Recently, new therapeutic strategies have been designed to target CICs and the tumour niche [51,52]. Our study reveals that TLR4⁺ luminal breast cancer cells express higher levels of ALDH1A1, and that only co-injection of the TLR4⁺ tumour cells and CAFs have the capacity to form tumours in mice, suggesting that TLR4 is a marker of BCICs. Thus, autophagic CAFs in the breast cancer microenvironment mediate the exocytosis of HMGB1, which activates its receptor TLR4 on luminal breast cancer cells to facilitate the expansion of BCICs (Figure 6D). Thus, both autophagy in CAFs and TLR4 on luminal breast cancer cells may serve as therapeutic targets and prognostic markers in luminal breast cancer patients.

Supplementary Material

Refer to Web version on PubMed Central for supplementary material.

Acknowledgements

The authors thank Mrs Wei Sun and Li-Ting Wang (Central Laboratory, Third Military Medical University, Chongqing, PR China) for technical assistance with laser confocal scanning microscopy. The authors also thank their colleagues for helpful comments. This project was supported by grants from the key project of National Natural Science Foundation of China (No. 81230062 to X-WB), the National Natural Science Foundation of China (No. 81372684 to X-HY), the National Key Research and Development Programme of China Stem Cell and Translational Research (2016YFA0101203 to X-WB), and the open project supported by Key Laboratory of Tumour Immunopathology, Ministry of Education of China (No. 2015jszl07 to X-HY).

References

1. Egeblad M, Nakasone ES, Werb Z. Tumors as organs: complex tissues that interface with the entire organism. *Dev Cell* 2010; 18: 884–901. [PubMed: 20627072]
2. Antoniou A, Hébrant A, Dom G, et al. Cancer stem cells, a fuzzy evolving concept: a cell population or a cell property? *Cell Cycle* 2014; 50: 3743–3748.
3. Joyce JA, Pollard JW. Microenvironmental regulation of metastasis. *Nat Rev Cancer* 2009; 9: 239–252. [PubMed: 19279573]
4. Reya T, Morrison SJ, Clarke MF, et al. Stem cells, cancer, and cancer stem cells. *Nature* 2001; 414: 105–111. [PubMed: 11689955]
5. McCarthy N. Enforced compliance. *Nat Rev Cancer* 2012; 12: 152.
6. Mitra S, Stemke-Hale K, Mills GB, et al. Interactions between tumor cells and microenvironment in breast cancer: a new opportunity for targeted therapy. *Cancer Sci* 2012; 103: 400–407. [PubMed: 22151725]
7. Vaiopoulos AG, Kostakis ID, Koutsilieris M, et al. Colorectal cancer stem cells. *Stem Cells* 2012; 30: 363–371. [PubMed: 22232074]
8. Malanchi I, Santamaria-Martinez A, Susanto E, et al. Interactions between cancer stem cells and their niche govern metastatic colonization. *Nature* 2011; 481: 85–89. [PubMed: 22158103]
9. Charafe-Jauffret E, Ginestier C, Iovino F, et al. Breast cancer cell lines contain functional cancer stem cells with metastatic capacity and a distinct molecular signature. *Cancer Res* 2009; 69: 1302–1313. [PubMed: 19190339]
10. Ginestier C, Hur MH, Charafe-Jauffret E, et al. ALDH1 is a marker of normal and malignant human mammary stem cells and a predictor of poor clinical outcome. *Cell Stem Cell* 2007; 1: 555–567. [PubMed: 18371393]
11. Busch S, Acar A, Magnusson Y, et al. TGF-beta receptor type-2 expression in cancer-associated fibroblasts regulates breast cancer cell growth and survival and is a prognostic marker in premenopausal breast cancer. *Oncogene* 2015; 34: 27–38. [PubMed: 24336330]
12. Polanska UM, Orimo A. Carcinoma-associated fibroblasts: non-neoplastic tumour-promoting mesenchymal cells. *J Cell Physiol* 2013; 228: 1651–1657. [PubMed: 23460038]
13. Chen WJ, Ho CC, Chang YL, et al. Cancer-associated fibroblasts regulate the plasticity of lung cancer stemness via paracrine signalling. *Nat Commun* 2014; 5: 3472. [PubMed: 24668028]
14. Tsuyada A, Chow A, Wu J, et al. CCL2 mediates cross-talk between cancer cells and stromal fibroblasts that regulates breast cancer stem cells. *Cancer Res* 2012; 72: 2768–2779. [PubMed: 22472119]
15. Gong C, Bauvy C, Tonelli G, et al. Beclin 1 and autophagy are required for the tumorigenicity of breast cancer stem-like/progenitor cells. *Oncogene* 2013; 32: 2261–2272. [PubMed: 22733132]
16. Yue W, Hamai A, Tonelli G, et al. Inhibition of the autophagic flux by salinomycin in breast cancer stem-like/progenitor cells interferes with their maintenance. *Autophagy* 2013; 9: 714–729. [PubMed: 23519090]
17. Galavotti S, Bartesaghi S, Faccenda D, et al. The autophagy-associated factors DRAM1 and p62 regulate cell migration and invasion in glioblastoma stem cells. *Oncogene* 2013; 32: 699–712. [PubMed: 22525272]
18. Lefort S, Joffre C, Kieffer Y, et al. Inhibition of autophagy as a new means of improving chemotherapy efficiency in high-LC3B triple-negative breast cancers. *Autophagy* 2014; 10: 2122–2142. [PubMed: 25427136]

19. Deretic V, Jiang S, Dupont N. Autophagy intersections with conventional and unconventional secretion in tissue development, remodeling and inflammation. *Trends Cell Biol* 2012; 22: 397–406. [PubMed: 22677446]
20. Nickel W, Rabouille C. Mechanisms of regulated unconventional protein secretion. *Nat Rev Mol Cell Biol* 2009; 10: 148–155. [PubMed: 19122676]
21. Zhang M, Schekman R. Cell biology. Unconventional secretion, unconventional solutions. *Science* 2013; 340: 559–561. [PubMed: 23641104]
22. Capparelli C, Guido C, Whitaker-Menezes D, et al. Autophagy and senescence in cancer-associated fibroblasts metabolically supports tumor growth and metastasis via glycolysis and ketone production. *Cell Cycle* 2012; 11: 2285–2302. [PubMed: 22684298]
23. Goldhirsch A, Wood WC, Coates AS, et al. Strategies for subtypes – dealing with the diversity of breast cancer: highlights of the St Gallen International Expert Consensus on the Primary Therapy of Early Breast Cancer 2011. *Ann Oncol* 2011; 22: 1736–1747. [PubMed: 21709140]
24. Dontu G, Abdallah WM, Foley JM, et al. In vitro propagation and transcriptional profiling of human mammary stem/progenitor cells. *Genes Dev* 2003; 17: 1253–1270. [PubMed: 12756227]
25. Mani SA, Guo W, Liao MJ, et al. The epithelial–mesenchymal transition generates cells with properties of stem cells. *Cell* 2008; 133: 704–715. [PubMed: 18485877]
26. Wang B, Wang Q, Wang Z, et al. Metastatic consequences of immune escape from NK cell cytotoxicity by human breast cancer stem cells. *Cancer Res* 2014; 74: 5746–5757. [PubMed: 25164008]
27. Yang Y, Liu Y, Yao X, et al. Annexin 1 released by necrotic human glioblastoma cells stimulates tumor cell growth through the formyl peptide receptor 1. *Am J Pathol* 2011; 179: 1504–1512. [PubMed: 21782780]
28. Naito S, von Eschenbach AC, Giavazzi R, et al. Growth and metastasis of tumor cells isolated from a human renal cell carcinoma implanted into different organs of nude mice. *Cancer Res* 1986; 46: 4109–4115. [PubMed: 3731078]
29. Babalonis S, Lofwall MR, Nuzzo PA, et al. Autophagy: assays and artifacts. *J Pathol* 2010; 221: 117–124. [PubMed: 20225337]
30. Muller S, Scaffidi P, Degryse B, et al. New EMBO members’ review: the double life of HMGB1 chromatin protein: architectural factor and extracellular signal. *EMBO J* 2001; 20: 4337–4340. [PubMed: 11500360]
31. Ohnishi M, Monda A, Takemoto R, et al. High-mobility group box 1 up-regulates aquaporin 4 expression via microglia–astrocyte interaction. *Neurochem Int* 2014; 75: 32–38. [PubMed: 24893328]
32. Mollica L, De Marchis F, Spitaleri A, et al. Glycyrrhizin binds to high-mobility group box 1 protein and inhibits its cytokine activities. *Chem Biol* 2007; 14: 431–441. [PubMed: 17462578]
33. Ogiku M, Kono H, Hara M, et al. Glycyrrhizin prevents liver injury by inhibition of high-mobility group box 1 production by Kupffer cells after ischemia–reperfusion in rats. *J Pharmacol Exp Ther* 2011; 339: 93–98. [PubMed: 21737537]
34. Yamaguchi H, Kidachi Y, Kamiie K, et al. Structural insight into the ligand–receptor interaction between glycyrrhetic acid (GA) and the high-mobility group protein B1 (HMGB1)–DNA complex. *Bioinformatics* 2012; 8: 1147–1153. [PubMed: 23275711]
35. Matsunaga N, Tsuchimori N, Matsumoto T, et al. TAK-242 (resatorvid), a small-molecule inhibitor of Toll-like receptor (TLR) 4 signaling, binds selectively to TLR4 and interferes with interactions between TLR4 and its adaptor molecules. *Mol Pharmacol* 2011; 79: 34–41. [PubMed: 20881006]
36. White E. Deconvoluting the context-dependent role for autophagy in cancer. *Nat Rev Cancer* 2012; 12: 401–410. [PubMed: 22534666]
37. Kantara C, O’Connell M, Sarkar S, et al. Curcumin promotes autophagic survival of a subset of colon cancer stem cells, which are ablated by DCLK1-siRNA. *Cancer Res* 2014; 74: 2487–2498. [PubMed: 24626093]
38. Nakayama S, Torikoshi Y, Takahashi T, et al. Prediction of paclitaxel sensitivity by CDK1 and CDK2 activity in human breast cancer cells. *Breast Cancer Res* 2009; 11: R12. [PubMed: 19239702]

39. Genevieve D, Jessica V, Ashleigh U, et al. Low dose, low cost estradiol pellets can support MCF-7 tumour growth in nude mice without bladder symptoms. *J Cancer* 2015; 6: 1331–1336. [PubMed: 26640593]
40. Rabouille C, Malhotra V, Nickel W. Diversity in unconventional protein secretion. *J Cell Sci* 2012; 125: 5251–5255. [PubMed: 23377655]
41. Tang D, Kang R, Livesey KM, et al. Endogenous HMGB1 regulates autophagy. *J Cell Biol* 2010; 190: 881–892. [PubMed: 20819940]
42. Apetoh L, Ghiringhelli F, Tesniere A, et al. The interaction between HMGB1 and TLR4 dictates the outcome of anticancer chemotherapy and radiotherapy. *Immunol Rev* 2007; 220: 47–59. [PubMed: 17979839]
43. Curtin JF, Liu N, Candolfi M, et al. HMGB1 mediates endogenous TLR2 activation and brain tumor regression. *PLoS Med* 2009; 6: e10. [PubMed: 19143470]
44. Yu M, Wang H, Ding A, et al. HMGB1 signals through toll-like receptor (TLR) 4 and TLR2. *Shock* 2006; 26: 174–179. [PubMed: 16878026]
45. Tian J, Avalos AM, Mao SY, et al. Toll-like receptor 9-dependent activation by DNA-containing immune complexes is mediated by HMGB1 and RAGE. *Nat Immunol* 2007; 8: 487–496. [PubMed: 17417641]
46. Campana L, Bosurgi L, Rovere-Querini P. HMGB1: a two-headed signal regulating tumor progression and immunity. *Curr Opin Immunol* 2008; 20: 518–523. [PubMed: 18599281]
47. Dong Xda E, Ito N, Lotze MT, et al. High mobility group box I (HMGB1) release from tumor cells after treatment: implications for development of targeted chemoimmunotherapy. *J Immunother* 2007; 30: 596–606. [PubMed: 17667523]
48. Bustin M At the crossroads of necrosis and apoptosis: signaling to multiple cellular targets by HMGB1. *Sci STKE* 2002; 2002: pe39. [PubMed: 12297673]
49. Perou CM, Sorlie T, Eisen MB, et al. Molecular portraits of human breast tumours. *Nature* 2000; 406: 747–752. [PubMed: 10963602]
50. Sorlie T, Perou CM, Tibshirani R, et al. Gene expression patterns of breast carcinomas distinguish tumor subclasses with clinical implications. *Proc Natl Acad Sci U S A* 2001; 98: 10869–10874. [PubMed: 11553815]
51. Plaks V, Kong N, Werb Z. The cancer stem cell niche: how essential is the niche in regulating stemness of tumor cells? *Cell Stem Cell* 2015; 16: 225–238. [PubMed: 25748930]
52. Vermeulen L, de Sousa e Melo F, Richel DJ, et al. The developing cancer stem-cell model: clinical challenges and opportunities. *Lancet Oncol* 2012; 13: e83–e89. [PubMed: 22300863]

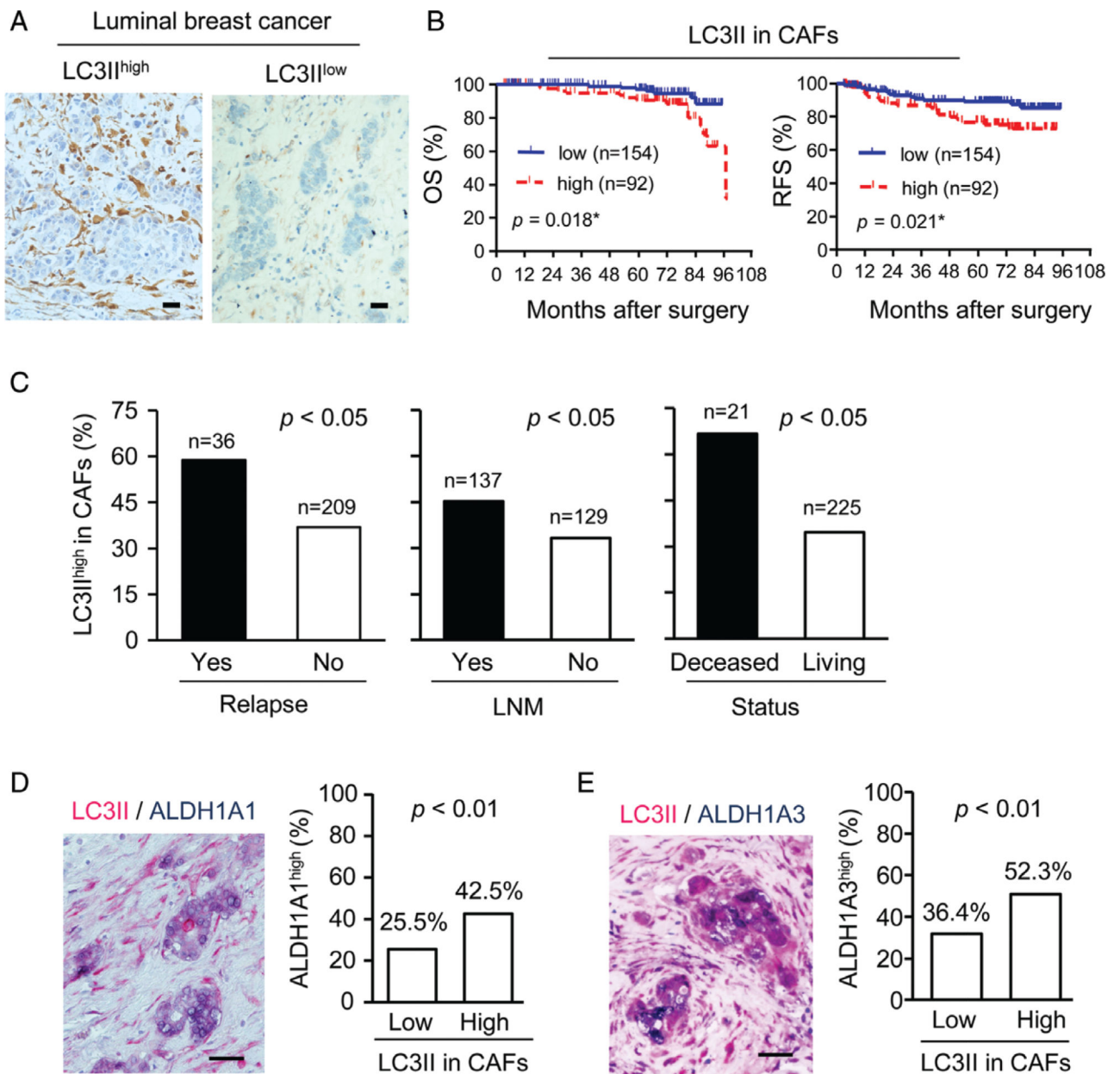


Figure 1. The correlation between LC3II in CAFs and prognosis of luminal breast cancer patients. (A) Representative immunohistochemistry of LC3II in CAFs of luminal breast cancer. LC3II localizes to the cytoplasm (brown colour). Scale bar: 100 μ m. (B) OS and RFS rates in patients divided into LC3II^{low} and LC3II^{high} expression in CAFs. (C) Relapse, LNM and survival status of patients with LC3II^{high} expression in CAFs. (D) Representative double-staining of LC3II (red) and ALDH1A1 (blue) in luminal breast cancer specimens (left panel) and quantification (right panel; $n=303$). (E) Representative double-staining of LC3II (red) and ALDH1A3 (blue) in luminal breast cancer specimens (left panel) and quantification ($n=303$) (right panel).

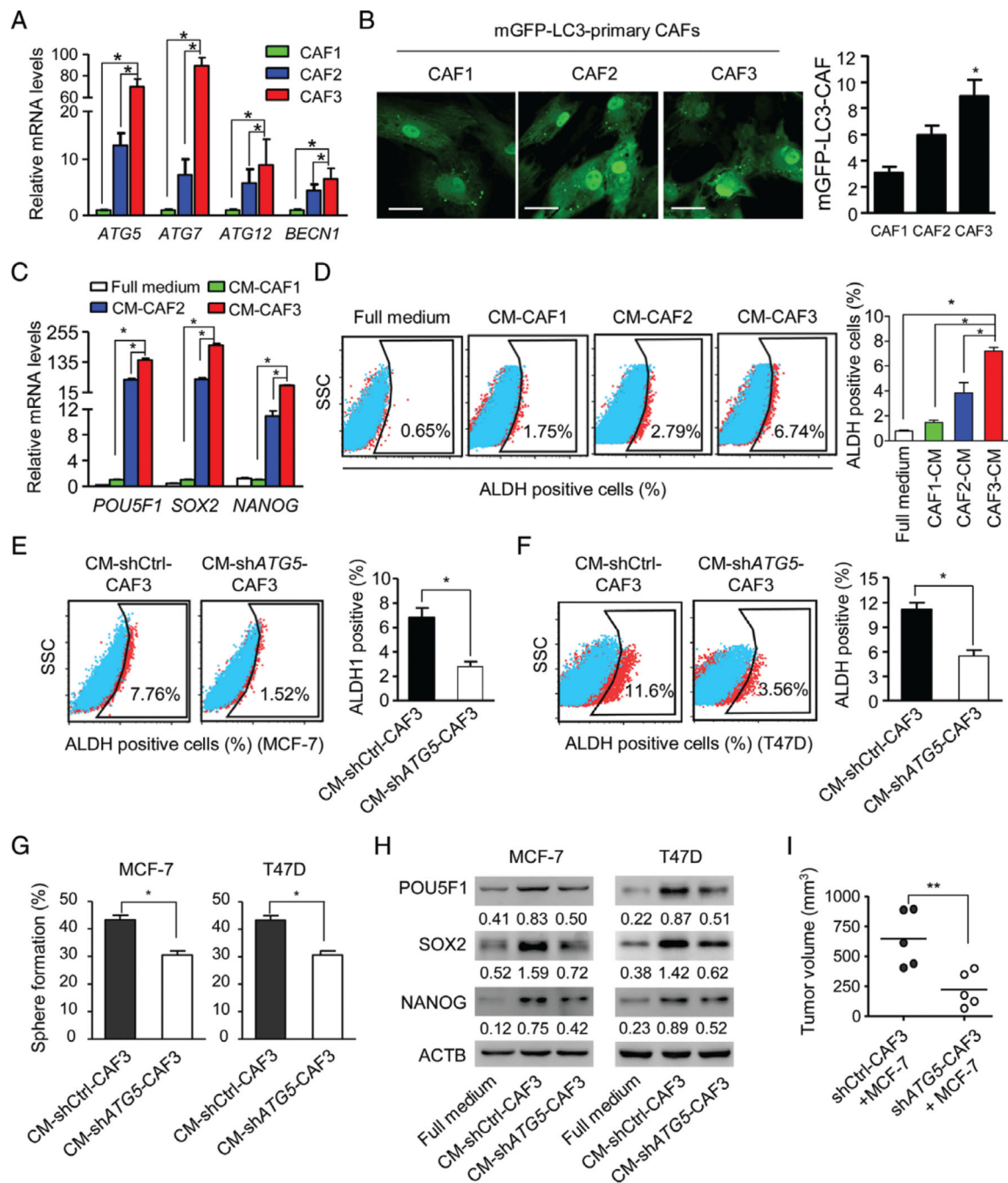


Figure 2. Autophagic CAFs enhance the stemness of luminal breast cancer cells. (A) Quantitative RT-PCR of autophagy gene mRNAs in primary CAFs (CAF1, CAF2, and CAF3) isolated from luminal breast cancers in serum-free medium for 24 h. (B) Primary CAFs transfected with mGFP-LC3 were cultured in serum-free medium for 24 h. Confocal microscopy was used to assess autophagy, as shown by green spots (left panel). Sixty cells were randomly chosen for counting of the number of mGFP-LC3 fluorescent spots per CAF (right panel). Scale bar: 50 μ m. (C) The mRNA levels of the stem cell marker genes *POU5F*, *SOX2* and *NANOG* in

MCF-7 luminal breast cancer cells cultured with full medium and supernatants from CAF1, CAF2 and CAF3 in serum-free medium (CM-CAF). (D) ALDH⁺ cells examined by flow cytometry in MCF-7 cells in full medium and CM-CAFs. (E, F) ALDH activity in MCF-7 and T47D cells cultured in CM from shCtrl-CAF3 (CM-shCtrl-CAF3) and shATG5-CAF3 (CM-shATG5-CAF3). (G) Sphere-forming capabilities of MCF-7 and T47D cells cultured in CM-shCtrl-CAF3 or CM-shATG5-CAF3. (H) Western blots of POU5F1, SOX2 and NANOG in MCF-7 and T47D cells cultured in full medium, CM-shCtrl-CAF3, and CM-shATG5-CAF3. (I) Co-injection of MCF-7 cells with shCtrl-CAF3 or shATG5-CAF3 into the mammary pads of NOD-SCID mice. Tumours were collected 4 weeks after implantation. Dot plots show tumour volumes ($n = 5$ mice in each group). * $P < 0.05$; ** $P < 0.01$.

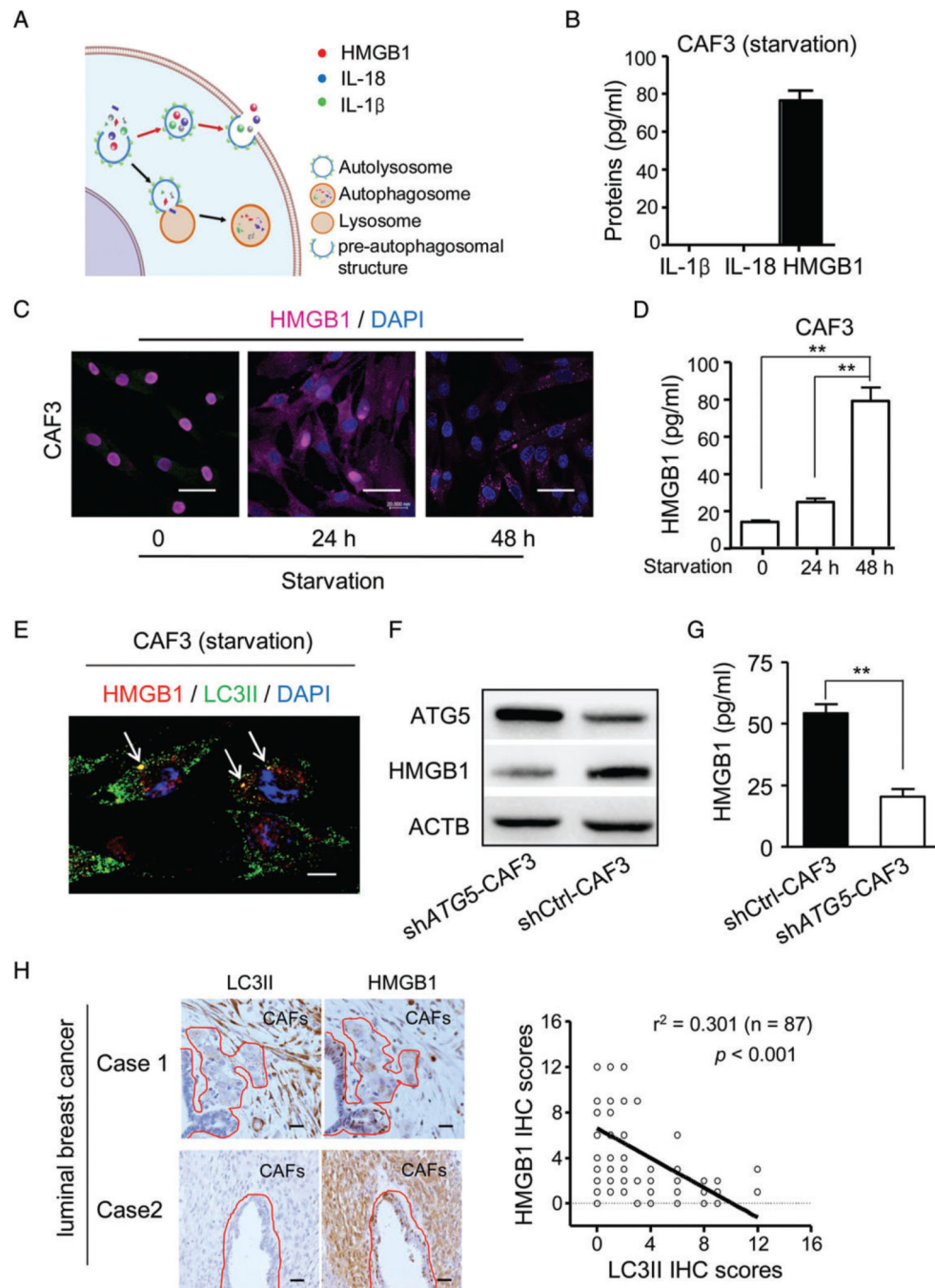


Figure 3.

HMGB1 is secreted by autophagic CAFs in luminal breast cancer. (A) The route of autosecretion. (B) ELISAs for IL-1 β , IL-18 and HMGB1 in the supernatants from CAF3 ($2.3 \times 10^5/2$ ml) cultured with serum-free medium (starvation) for 48 h. (C) Immunofluorescence of HMGB1 in CAF3 cultured with serum-free medium (starvation) for 0, 24 and 48 h. Purple: HMGB1. Blue: nucleus. Scale bar: 50 μ m. (D) ELISA for HMGB1 in the supernatants from CAF3 ($2.3 \times 10^5/2$ ml) with serum-free medium (starvation) for 0, 24 and 48 h ($n = 6$). (E) Co-localization of HMGB1 (red) with LC3II (green) in CAF3

cultured with serum-free medium. Nuclei are stained blue. White arrows: co-localization of HMGB1 with LC3II (yellow). Scale bar: 10 μm . (F) Western blot of ATG5 and HMGB1 in shATG5-CAF3 and shCtrl-CAF3 cultured with serum-free medium for 48 h. (G) ELISA of HMGB1 in the supernatants from CAF3-shCtrl and CAF3-shATG5 ($2.1 \times 10^5/2$ ml) with serum-free medium for 48 h ($n= 6$). (H) IHC of HMGB1 and LC3II in representative serial sections of luminal breast cancer specimens (left panel). Areas surrounded by the red lines represent breast cancer cells. Scale bar: 100 μm . Associations between scores of HMGB1 and LC3II assessed by linear regression and the *F*-test in 87 specimens (right panel). ** $P < 0.01$. DAPI, 4',6-diamidino-2-phenylindole.

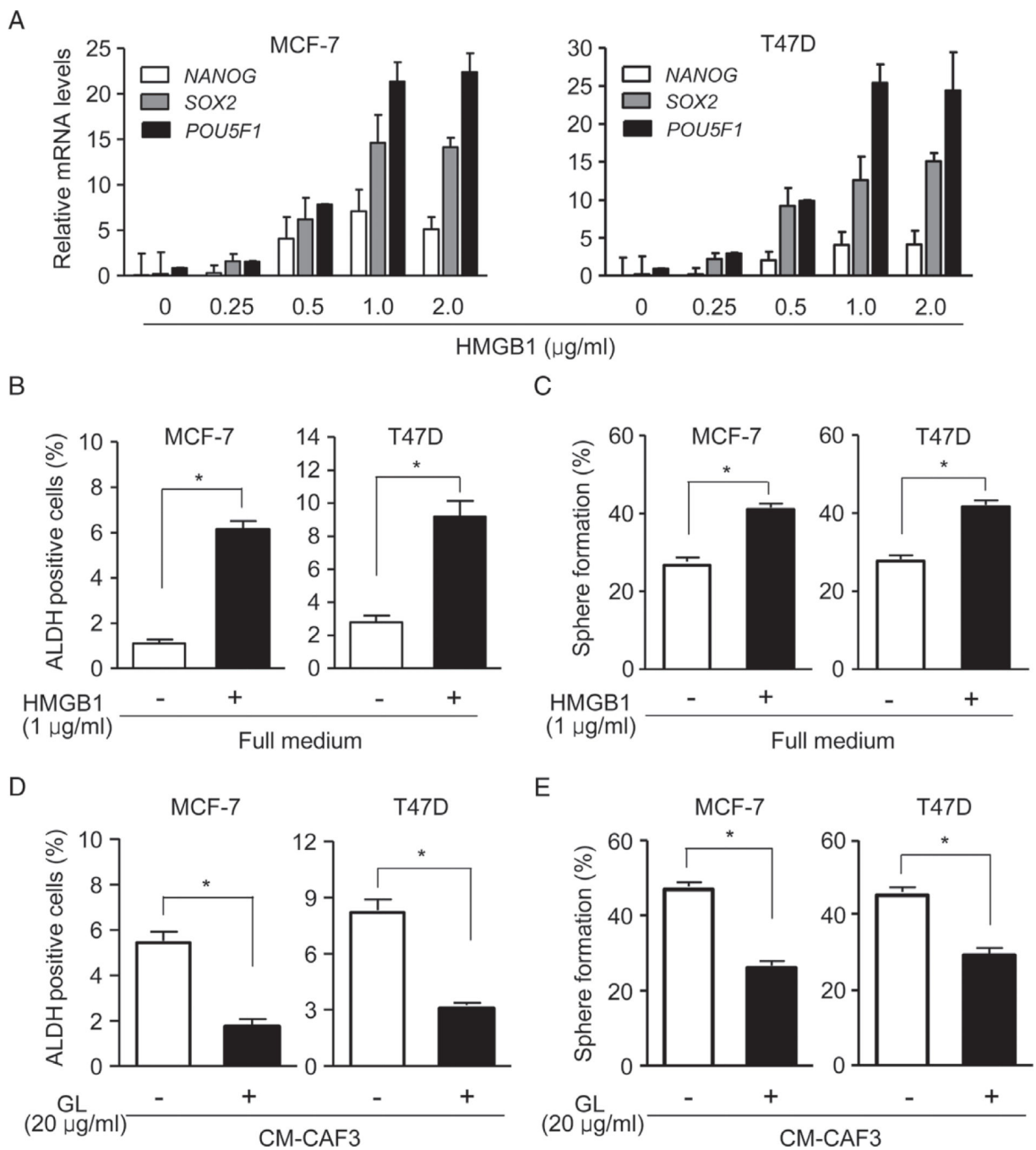


Figure 4. HMGB1 maintains stemness. (A) The mRNA levels of the stem cell marker genes *POU5F1*, *SOX2* and *NANOG* in MCF-7 (left panel) and T47D (right panel) cells treated with the indicated concentrations of HMGB1. (B and C) Flow cytometry for ALDH activity (B) and sphere formation (C) by MCF-7 and T47D cells treated with or without 1 μg/ml HMGB1. (D and E) ALDH activity (D) and sphere formation (E) by MCF-7 and T47D cells with or without 20 μg/ml GL in CM-CAF3. * $P < 0.05$.

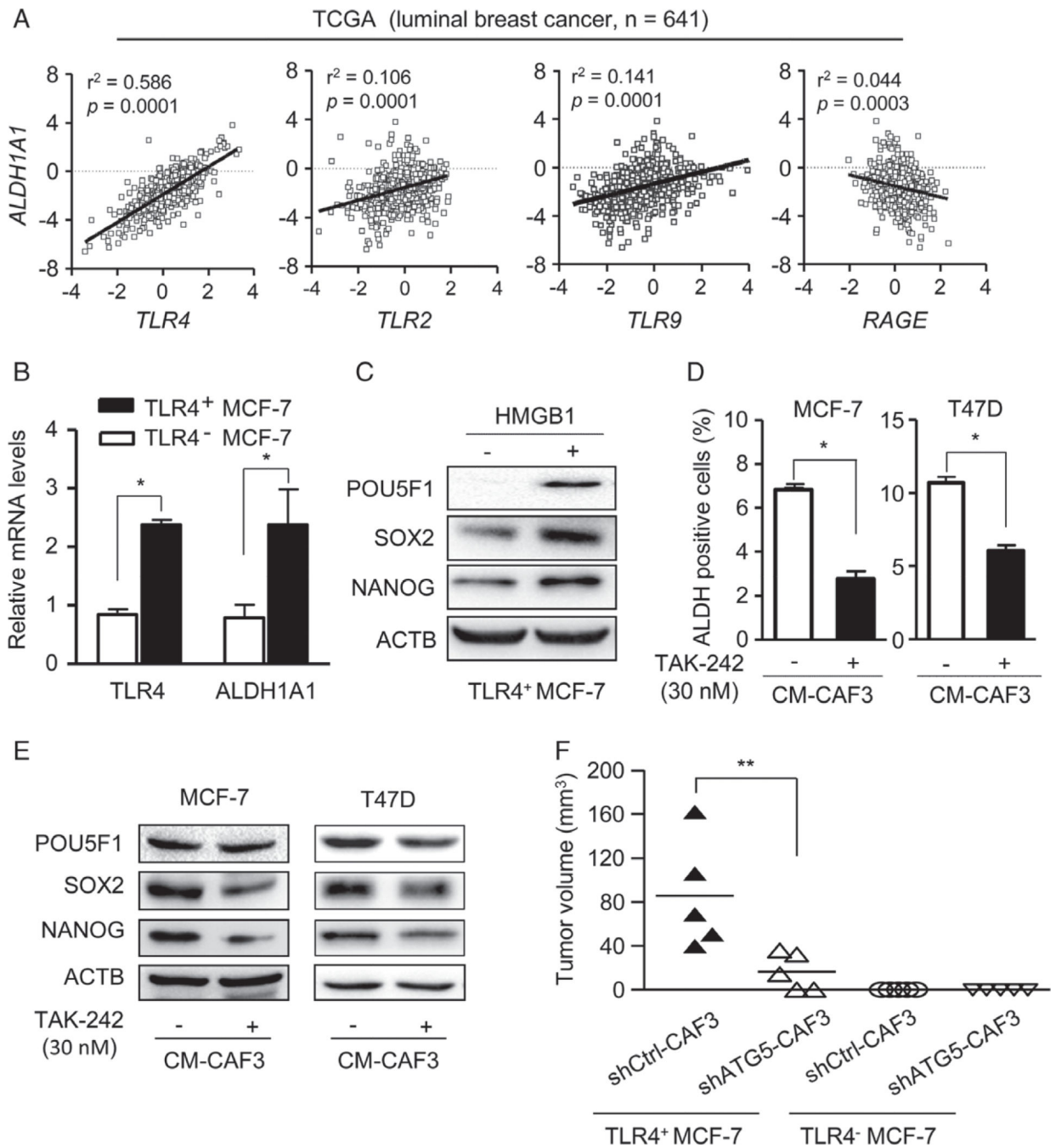


Figure 5.

TLR4 in cancer cells mediates the cross-talk between autophagic CAFs and BCICs. (A) Correlation between *ALDH1* and HMGB1 receptor (*TLR4*, *TLR2*, *TLR9* and *RAGE*) mRNA levels in luminal breast cancer ($n = 641$, TCGA). Statistical significance was determined by linear regression and the *F*-test. (B) *TLR4* and *ALDH1A1* mRNA levels in TLR4⁺ and TLR4⁻ MCF-7 cells. (C) The levels of POU5F1, SOX2 and NANOG in TLR4⁺ cells with or without 1 μ g/ml HMGB1. (D) ALDH⁺ MCF-7 and T47D cells in CM-CAF3 with or without 30 nM TAK-242. (E) Western blots of POU5F1, SOX2 and NANOG in

MCF-7 and T47D cells in CM-CAF3 with or without TAK-242 (30 nM). (F) Tumour volumes in mice with mammary pad injection of TLR4⁺ and TLR4⁻ MCF-7 cells with or without CAF3 transfected with shCtrl or sh*ATG5* measured 2 weeks after implantation (*n*= 5 mice per group). ***P* < 0.01.

Author Manuscript

Author Manuscript

Author Manuscript

Author Manuscript

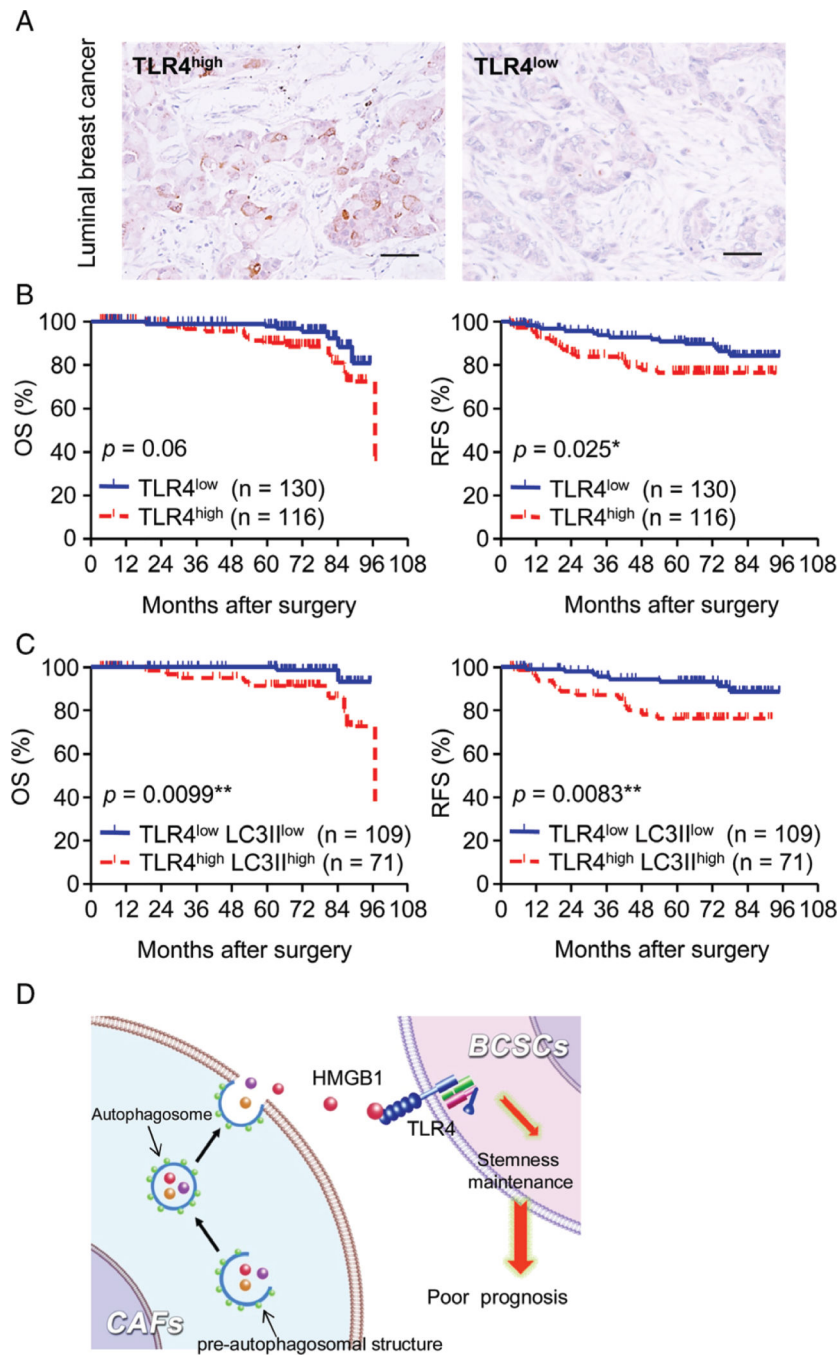


Figure 6. Levels of LC3II in CAFs and TLR4 on cancer cells are associated with poor prognosis of luminal breast cancer patients. (A) Representative IHC staining of TLR4 in cancer cells. Scale bar: 100 μ m. (B) Kaplan–Meier estimation of OS and RFS rates in TLR4^{high} and TLR4^{low} groups of luminal breast cancers. (C) Patients were divided into LC3II^{high}/TLR4^{high} and LC3II^{low}/TLR4^{low} groups by combining the levels of LC3II in CAFs and TLR4 in cancer cells. (D) Schematic representation of the cross-talk between CAFs and

BCICs in luminal breast cancer. Autophagic CAFs secrete HMGB1 to activate TLR4 on BCICs to maintain stemness.

Author Manuscript

Author Manuscript

Author Manuscript

Author Manuscript